A Quantitative Method to Determine ICT Delay Requirements for Wide-Area Power System Damping Controllers

Nguyen Tuan Anh, Luigi Vanfretti, *Senior Member, IEEE*, Johan Driesen, *Senior Member, IEEE*, and Dirk Van Hertem, *Senior Member, IEEE*

***Abstract*—This paper presents a quantitative method to determine delay requirements of the information and communication technology (ICT) system supporting wide-area power oscillation damping (WAPOD) controllers. An allowable time delay for the ICT infrastructure named "equivalent time delay (ETD)" is defined. The ETD is calculated by numerically comparing the damping behavior of the system when local input signals (LI) and remote input signals (RI) are used in the damping controller. The use of a WAPOD is only justified when its response outperforms that of a controller using local inputs. Therefore, the total time delay in the control loop must be below the calculated ETD. As such, the ETD serves as a design criteria to determine ICT latency requirements. The selection of an effective RI signal can be carried out by considering the maximum delays (ETDs) of different wide-area measurements. A damping improvement $\mathbf{ETD}^{\alpha\ \%}$ has been proposed using the same methodology indicating a minimum outperformance of the remote signals. The proposed method is demonstrated using the well-known Klein-Rogers-Kundur multi-machine power system and the Vietnamese power system model.**

***Index Terms*—Information and communication technology (ICT) delay, phasor measurements unit (PMU), power systems, synchrophasors, wide-area control system (WACS), wide-area damping controller.**

I. Introduction

ACTUAL power systems have numerous electro-mechanical oscillation modes. These modes can represent local or inter-area interactions between synchronous machines. Low frequency inter-area oscillations (0.1–1.0 Hz) are influenced by global states of large machine clusters in the power network, and they are more difficult to control and damp [1], [2]. The traditional approach to add damping is the use of a power oscillation damping (POD) controller to a controllable device, such as the exciter of a synchronous machine (i.e., PSS), or a FACTS device. Generally, these devices make use of local input (LI) signals, and they are ideally suited to dampen local oscillation modes. However, they may not be effective in dealing with inter-area oscillations, because such modes may not be observable in the available LI signals, or because these active devices might not provide sufficient controllability to a specific mode [3]. Alternatively, power oscillation damping can be achieved through the use of the most suitable (remote) input signals (RI) and active devices placed at a location with high controllability to optimally dampen inter-area modes and to enhance the overall system stability [2], [4]–[10].

The use of remote signals leads to increased costs and might require coordination for real-time data exchange between power system operators. This is necessary to assure that communication loss does not lead to additional reliability issues. Local input signals require fewer and simpler equipment. As a consequence, the use of RI is only justified if the resulting stability enhancement outperforms that of the LI signal, and preferably with a margin.

Remote input signals require the use of time synchronized measurements, which are transferred via communication links to a wide-area control system (WACS). WACS includes an ICT platform that merges the input data and transforms it to a useful input signal for active devices. WACS consists of 1) a number of synchronized phasor measurements units (PMUs) from geographically spread locations, 2) a computer system termed phasor data concentrator (PDC), 3) a real-time computer system where control functions are implemented, and 4) a communication network [11], [12]. Although WACS are designed considering communication latency, signal propagation in communication links and processing time in the ICT system result in an unavoidable end-to-end time delay that may surpass latency bounds considered in the design of WACS. The delays can vary from tens of milliseconds up to several hundreds of milliseconds. The delay depends on the distance between remote measuring sites, the communication carrier, communication protocol and several other factors [13], [14]. Observe that the total delay in a control loop will not be constant due to the properties of packet switched networks [15].

Inter-area modes are predominantly determined by interactions between machine clusters, and as a result, signals from these clusters provide the best visibility of such modes [11].

Manuscript received March 17, 2014; revised July 16, 2014; accepted August 18, 2014. Date of publication September 23, 2014; date of current version June 16, 2015. The Electa group is a founding member of EnergyVille. This work was supported in part by the EIT InnoEnergy Smart Power project. The work of L. Vanfretti was supported by Statnett SF, the Nordic Transmission System Operator, the StandUP for Energy Collaboration Initiative, and by Nordic Energy Research through the Strong Grid project. Paper no. TPWRS-00379-2014.

N. T. Anh, J. Driesen, and D. Van Hertem are with the Electrical Engineering Department (research group Electa) of KU Leuven, Leuven, Belgium (e-mail: Anh.NguyenTuan@esat.kuleuven.be; Johan.Driesen@esat.kuleuven.be; Dirk.VanHertem@esat.kuleuven.be).

L. Vanfretti is with the Electric Power Systems Department of KTH Royal Institute of Technology, Stockholm, Sweden, and also with the R&D Division of Statnett SF, Oslo, Norway (e-mail: Luigi.Vanfretti@ee.kth.se; Luigi.vanfretti@statnett.no).

Digital Object Identifier 10.1109/TPWRS.2014.2356480

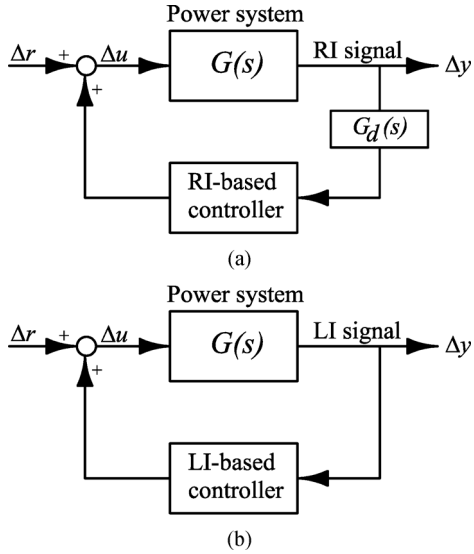

Fig. 1. Transfer function of closed-loop power system with a POD controller using: (a) RI signal and (b) LI signal.

For controllable devices such as SVCs and TCSCs, RI signals such as magnitudes or phase angle differences of key generator terminal voltages, or a combination of them (such as averaged bus angle differences), which are measured by PMUs, can have better observalility than LI signals [11], [16]. However, as ICT delay increases, the phase margin of the system decreases [15], and thus, this delay has a destabilizing effect which reduces the controllers' damping performance. If the ICT delay is beyond a certain threshold, the performance of the WAPOD controller reduces to a level which is lower than that of the controller using a LI signal. There exists an "equivalent time delay (ETD)" for which the damping behavior of the system using a LI control and RI control exhibit the same damping. This ETD can be used as a design criteria for the WACS. So far, there are no available systematic quantitative definitions or methods to put requirements on the ICT delay bounds that the WACS should meet for wide-area control applications.

This paper proposes the ETD and its application in setting requirements for ICT time delays in WACS applications in multi-machine power systems. The paper is structured as follows: Section II presents the ETD and its calculation method. ICT delay requirements are proposed in Section III. Sections IV and V show study results on a test system and an actual power system model. Conclusions are presented in Section VI.

II. Equivalent Time Delay (ETD)

Fig. 1 shows the closed-loop transfer function of a multi-machine system with a POD controller. $G(s)$ represents the open-loop transfer function of the power system. A damping controller can use either a RI or LI signal as input. A wide-area control system (WACS) provides raw PMU measurements to build the RI signal that controls the active device. The delay T_d associated with the WACS system is modeled by a transfer function $G_d(s)$. Within this paper, the Padé approximation is used [5].

The eigenvalue $\lambda_i = \sigma_i \pm j\omega_i$ is the ith eigenvalue of the linearized open-loop power system model. λ_i is a complex conjugate for each oscillation mode, which in this case corresponds to the inter-area mode with the lowest damping. If the controller uses the RI signal, the eigenvalue of the linearized closed-loop system shifts to λ_i^r corresponding to a damping ratio ζ_i^r. When the controller uses the LI signal, λ_i^l and ζ_i^l are respectively the inter-area eigenvalue and damping ratio of the linearized closed-loop system.

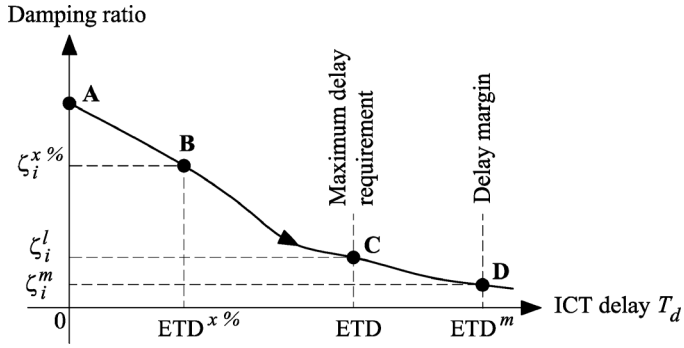

Fig. 2. Relationship between the wide-area controller's damping and WACS's delay.

A. ETD Definition

The ETD can be defined as the time delay, caused by the ICT system providing remote input signal to a feedback controller, which results in an equal damping performance for the system with RI and LI signals. *This definition assumes that the ETD is computed for a RI signal, which has larger modal observability than the LI signal.* RI signals with good modal observability can be derived using several methods such as the concept of dominant paths [17], residue analysis [18]–[20], damping torque analysis [21]–[23], and Hankel singular values (HSV) [24].

B. Derived Definitions

In a similar fashion, the delays shown in Fig. 2 are defined as follows:

$\text{ETD}^{x\,\%}$: which indicates the allowable time delay at which the RI signals have a damping ratio which is x % higher than when using the LI signals

ETD^m : which indicates the allowable time delay up to the stability margin.

C. ETD Calculation Method

Fig. 3 shows a flow chart for the ETD calculation. To define the ETD, the damping performance of both RI- and LI-based controllers is computed for each inter-area mode by determining ζ_i^r and ζ_i^l. Note that the wide-area controller's damping ζ_i^r depends on the ICT time delay T_d, and λ_i^r shifts to the right of the complex plane as T_d increases. Hence, an iterative method is used to define the ETD for a wide-area control signal. An initial value of T_d equal to zero is used to compute the initial eigenvalues of λ_i^r and λ_i^l as well as the damping ratios of ζ_i^r and ζ_i^l. If $\zeta_i^r > \zeta_i^l$, the time delay T_d is increased with a value ξ, and the damping ratios are re-computed. The iterative loop is repeated until the ETD is found at the point where $\zeta_i^r \simeq \zeta_i^l$.

The stepsize ξ is increased iteratively For this paper, a variable stepsize was used, from 100 ms up to 0.1 ms, each time reducing the stepsize by a factor of 10 after passing the ETD.

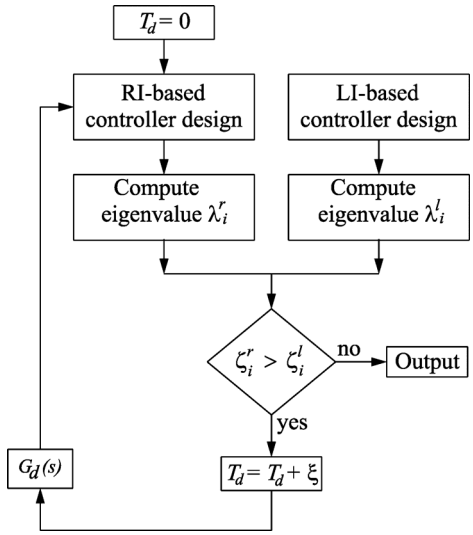

Fig. 3. Flow chart for ETD computation.

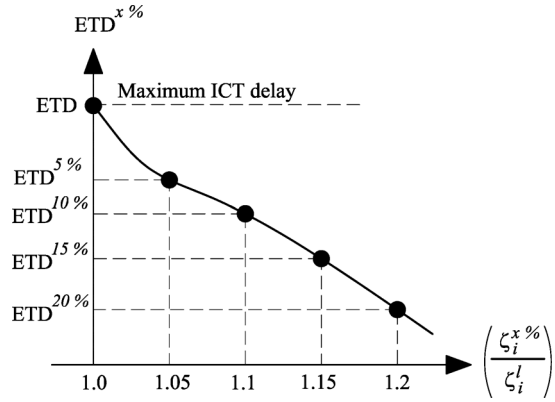

Fig. 4. Relation between damping enhancement and delay requirement.

III. ICT Delay Requirements

A. Maximum Delay

Fig. 2 illustrates the relation between the damping ratio ζ_i^r in a system using RI signals and the ICT time delay T_d. In the figure, point **A** corresponds to the maximum damping level at zero delay. When the delay increases to the ETD (point **C**), the damping reduces to the same level as the LI-based controller's damping ratio ζ_i^l. Point D (stability margin ζ_i^m) shown in [8], corresponds to a delay margin ETD^m, which allows the closed-loop power system to remain marginally stable.

The delay T_d of a practical WACS must be at least smaller than the ETD^m (point **D**) to guarantee stability, and smaller than the calculated ETD (point **C**) in order to outperform the response of the controller using local input signals.

B. Required Delay for Damping Improvement

At a minimum, it is required that the performance of the wide-area controller is equal to that of the system with LI signals. In addition, to justify investments and exploit the WACS system properly, the ICT system must provide a delay allowing the controller to attain a certain damping improvement over the system with LI signal. $\zeta_i^{x\,\%}$ is defined as the improved damping required to provide $x\,\%$ of damping enhancement compared to the local signal, and can be written as

$$\zeta_i^{x\,\%} = (1 + x) \cdot \zeta_i^l. \tag{1}$$

To ensure that the enhanced damping is attained, an ICT time delay ETD$^{x\,\%}$, corresponding to $\zeta_i^{x\,\%}$ must be determined. Fig. 4 illustrates the relationship between ETD$^{x\,\%}$ and damping improvement $(\zeta_i^{x\,\%}/\zeta_i^l)$. ETD$^{x\,\%}$ can be defined in a similar manner as the ETD calculation by setting ζ_i^l equal to $\zeta_i^{x\,\%}$.

C. ETDs for Different Wide-Area Signals

When we assume that the location of the active device (e.g., FACTS) is given, the damping effect of the wide-area controller depends mainly on the control signal. The ETD calculation brings an additional dimension to the selection of the most appropriate remote input signal. If the delay depends on the measurement location (e.g., because of the distance to the controller or available communication infrastructure), the ETD calculation can be integrated in the selection of the signal. When the ETDs are calculated for different inputs, the set of input signals with the highest ETD and highest damping enhancement result in the most adequate remote signal for the POD controller. This method is equivalent to a damping comparison of the controller using different signals with different levels of fixed ICT delay.

D. Delay Uncertainty

The ETD can be seen as the time delay that needs to be ensured by the communication system, and therefore defines the maximum acceptable time delay in the system. In case the communication delay is uncertain or variable, an uncertainty delay synchronization might be used which absorbs the uncertainty. In such a system, the ETD should be compared with the total delay, including the additional synchronization delay.

The time delay includes thus a fixed latency for signal processing algorithms to compute the phasors and a variable latency in data transmission on the communication infrastructure.

IV. Methodology Demonstration

A. Test System

This section demonstrates how the ETDs and ICT delay requirements for a WAPOD controller can be determined using the well-known Klein-Rogers-Kundur system [1], shown in Fig. 5. In steady-state, the system is heavily stressed with about 400 MW flows on the tie lines from Area 1 to Area 2 through the corridor between buses 7 and 9. A thyristor-controlled series capacitor (TCSC) with a POD controller is installed in the system to control the power flow in the corridor for stability improvement. As shown in the figure, a WACS is set up to provide wide-area measurements to the controller.

Similarly to [5], [16], and [25], the difference between the terminal voltage angles of generators 1 and 3, $(\angle \overrightarrow{V}_3 - \angle \overrightarrow{V}_1)$ is used as the TCSC controller's RI signal. For the controller using LI signals, the active power flowing through the line connecting buses 7 and 8 is chosen. Hence, the WACS must include two PMUs installed in buses 1 and 3, a PDC, the POD controller, and communication links provide the input signal for the damping

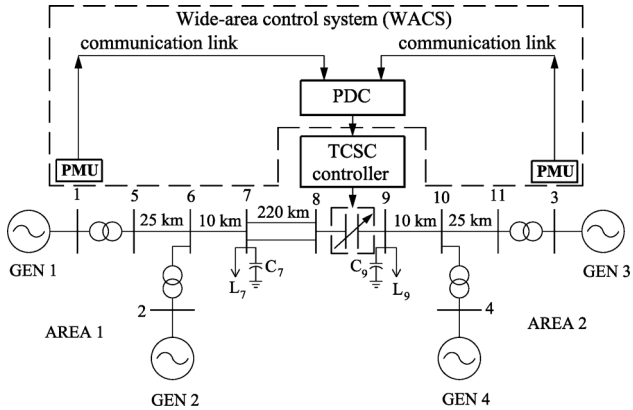

Fig. 5. Single line diagram of the test system.

TABLE I
LINEAR ANALYSIS RESULTS FOR THE TEST SYSTEM

	Eigenvalue of inter-area mode	Frequency (Hz)	Damping ratio
Without TCSC	$-0.104 \pm j3.367$	0.54	$\zeta_i^0 = 0.031$
TCSC controller using remote signal	$-0.615 \pm j3.586$	0.57	$\zeta_i^r = 0.169$
TCSC controller using local signal	$-0.388 \pm j3.449$	0.55	$\zeta_i^l = 0.112$
ETD (ms)	194		

controller. To calculate the ETD and delay requirements of the WACS, the damping performance of the controller using both RI and LI signals needs to be determined.

B. Determining ETD

Linear analysis of the open-loop system (without the TCSC modulation) is performed. A fixed series compensation of the line 7 – 8 equal to 20% is considered. The right eigenvectors (mode shapes) with respect to the rotor angle and speed states of the generators indicate an inter-area oscillation mode having the eigenvalue, frequency and damping ratio ζ_i^0 as shown in Table I. This mode corresponds to the inter-area oscillation of G1 and G2 against G3 and G4. The damping ratio of 0.031 should be improved to enhance system stability.

Closed-loop analysis with TCSC modulation is conducted, considering the controllers using RI and LI signals. The results are also shown in Table I. Fig. 6 shows the POD controller block diagram. The design of the POD controller of the TCSC (Fig. 6) consists of defining the lead-lag compensator and the gain [4], [26]. The proposed POD controller design includes two compensation stages, since the angle compensated by each block should not exceed 60° [4]. The parameters of the RI- and LI-based POD controllers are indicated in Table II. The time constants of the compensation blocks are determined using eigenvalue sensitivities with respect to the controller modulation. The controller gain of 0.3, selected for all RI- and LI-based controllers, was obtained using the root locus method and design specifications.

When the RI controller with a zero ICT delay is considered, the inter-area damping ratio ζ_i^r increases to 0.169. In the case of using the local signal, the controller has the damping ratio ζ_i^l of 0.112. Applying the proposed method, the calculated ETD is 194 ms, which gives the WACS's maximum allowable delay. If the delay is less than 194 ms, the wide-area controller will allow for a larger degree of damping performance enhancement than the controller using the LI signal.

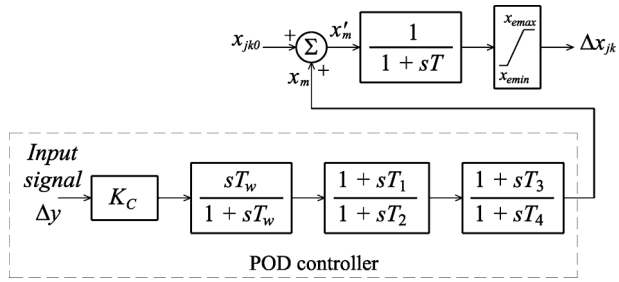

Fig. 6. Structure of the POD controller of the TCSC.

TABLE II
RI- AND LI-BASED CONTROLLER DESIGNS

	T	T_w	K_C	T_1 & T_3	T_2 & T_4
RI-based controller	0.05	1.5	0.3	0.5137	0.1717
LI-based controller	0.05	1.5	0.3	0.5059	0.1744

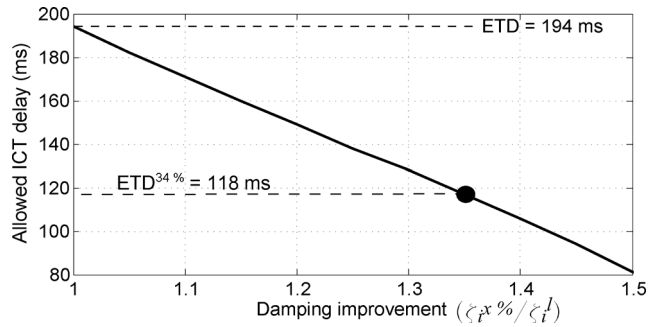

Fig. 7. ICT delays of the wide-area control system required for damping improvement.

C. Determining $\mathrm{ETD}^{x\,\%}$

In a next phase, the effect of having higher damping requirements for the RI controller is tested by varying ($x = \zeta_i^{x\,\%}/\zeta_i^l - 1$) from zero to 50%. The allowable delay $\mathrm{ETD}^{x\,\%}$ corresponding to these required damping levels are computed based on the method proposed in Section III-B. The results are shown in Fig. 7 as a curve of ICT delays versus the required damping improvement levels.

In some cases, a fixed system damping is specified, for instance $\zeta_i^r = 0.15$ [3]. This corresponds to a damping improvement of 34% over the LI based damping. In this case, the allowed ICT delay can be determined from Fig. 7 and is equal to 118 ms.

D. Selection of the RI Signal Based on ETD

Up to now, the phase angle difference between the bus voltages of nodes 1 and 3 was considered as the RI signal for the POD controller. However, a number of alternative input signals could be considered. For instance, the four available wide-area

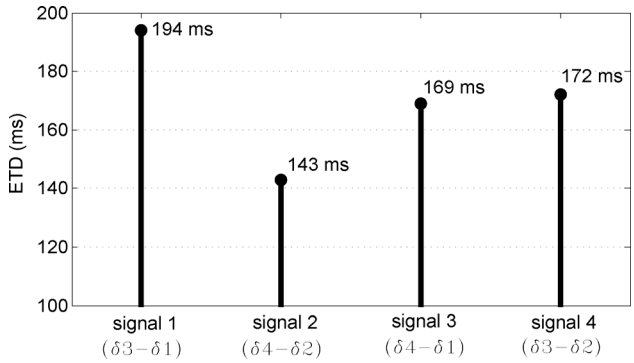

Fig. 8. ETDs for different wide-area measurements.

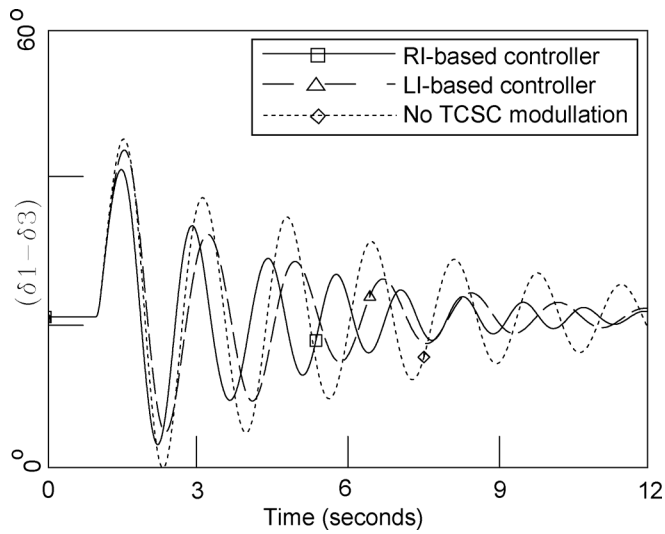

Fig. 9. Inter-area oscillation with and without the TCSC modulation. The ICT delay of the wide-area measurement is set to 194 ms.

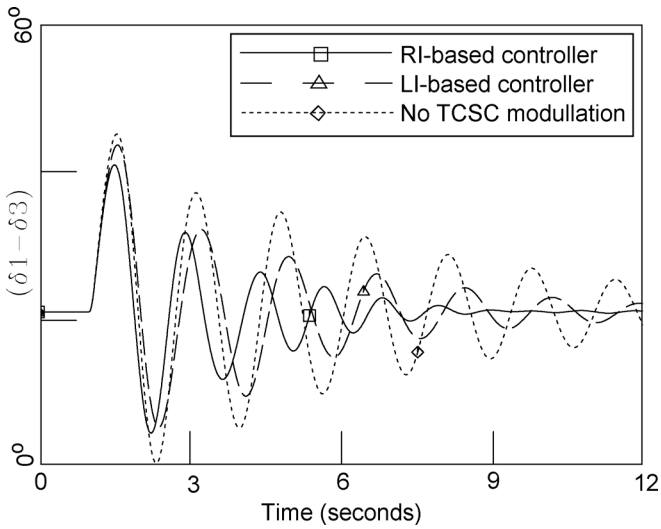

Fig. 10. Inter-area oscillation with and without the TCSC modulation. The ICT delay of the wide-area measurement is set to 118 ms.

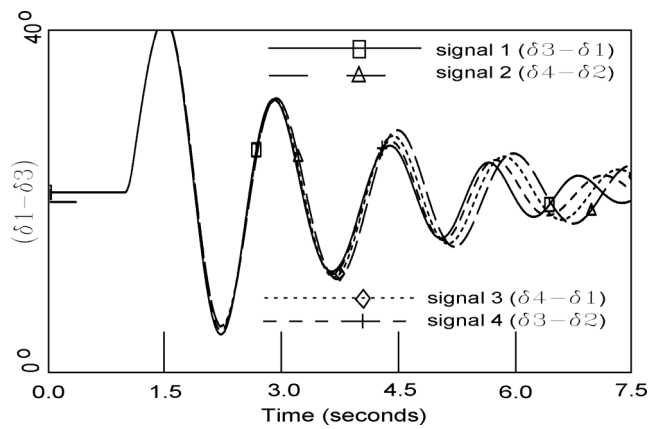

Fig. 11. Inter-area oscillation damping of the wide-area controller using different remote signals. The ICT delay of wide-area measurement is set to 118 ms.

signals of the terminal voltage angle differences of two generators: signal 1 ($\delta_3 - \delta_1$), signal 2 ($\delta_4 - \delta_2$), signal 3 ($\delta_4 - \delta_1$), and signal 4 ($\delta_3 - \delta_2$), are chosen to demonstrate a controller input signal selection using calculated ETDs. Fig. 8 shows a comparison of the calculated ETDs for these signals. Signal 1 ($\delta_3 - \delta_1$) is the most effective remote signal, because its ETD has the highest value (194 ms). Next is signal 4 ($\delta_3 - \delta_2$) with the ETD equal to 172 ms. This signal can be considered as an alternative or back-up signal.

In practical systems, the existing infrastructure might allow the use of an alternative input signal because of better/cheaper communication or installation costs. For instance, substation 2 might already have a PMU installed. A cost benefit analysis is needed to see whether the choice for the system with a lower performance outweighs the optimal (technical) solution.

E. Validation Through Nonlinear Simulations

Nonlinear simulations are used to test the controllers designed. It is assumed that in the system of Fig. 5, a three-phase to ground fault occurs on bus 7 and lasts for 100 ms. Fig. 9 shows the inter-area oscillations in the system in the case where the TCSC modulation is not active. These oscillations have low damping, and the damping performance needs to be enhanced.

Fig. 9 also shows the system response with the controllers using either a RI signal as $(\delta_3 - \delta_1)$, or a LI signal (active power). The delay of the wide-area measurement is set to 194 ms, the calculated ETD. The dynamic simulations show the response on the RI-based controller designed using the calculated ETD has similar damping to that of the controller using LI signal. Note that the time delay modeled by the Padé approximation causes a phase-lag between the RI and LI response. Therefore, applying an appropriate delay compensation method allows to enhance the damping performance of the WAPOD controller.

Damping improvement of the wide-area controller is shown in Fig. 10, when the ICT delay is taken as 118 ms. Note that at this latency, the controller using the remote signal stabilizes the inter-area oscillation more efficiently as compared to the local signal. This confirms that the damping has been enhanced for a required maximum allowed ETD$^{34\ \%}$.

A damping comparison of the controller using different wide-area measurements is illustrated in Fig. 11. The simulations again confirm the analysis carried out in the previous section, since signal 1 $(\delta_3 - \delta_1)$ is the most effective remote signal. If the ETD of a wide-area signal increases, the phase margin of the controller will increase, allowing for more series compensation [15].

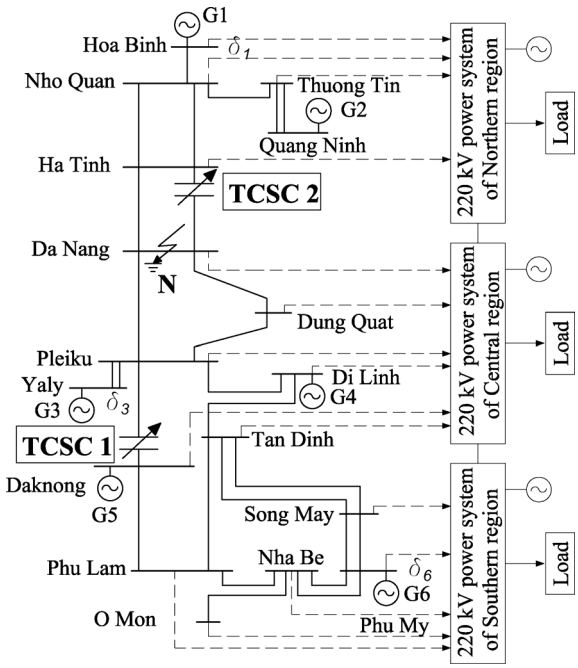

Fig. 12. Single-line diagram of the Vietnamese system.

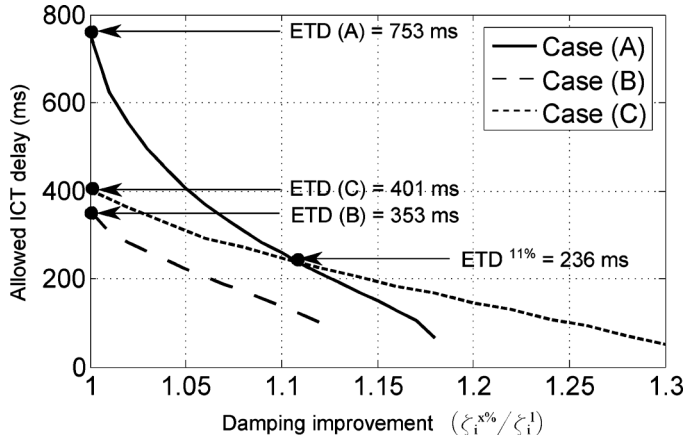

Fig. 13. Allowed ICT delays for the Vietnamese system.

TABLE III
LINEAR ANALYSIS RESULTS FOR THE VIETNAMESE SYSTEM

Case	Damping ratio		ETD
	ζ_i^l	ζ_i^r	(ms)
Without TCSC	0.154		
(A)	0.161	0.191	753
(B)	0.173	0.196	353
(C)	0.176	0.230	401

V. APPLICATION TO THE VIETNAMESE SYSTEM

A. Vietnamese Power System

The proposed method is applied to the current 220–500 kV power system of Vietnam. The power system model includes 153 generators of 51 power plants, in which 110 generators are in service. The system consists of 320 buses, 453 branches, and 174 transformers. The total installed capacity of power plants connected to the 220–500 kV system is 19 223 MW. We consider an operating condition, which corresponds to that of the raining season, when the total generation capacity is 13 528 MW, with a reserve margin of 42%. The total load is 13 293 MW. For simplicity and convenience in modal analysis, a 6-generators 16-buses equivalent model is reduced from the actual 153-generators 320-bus system [26]. Fig. 12 shows the single-line diagram of the 500 kV network (equivalent system). Note that the system can be divided into 3 areas (North, Central and South) represented by G1 and G2, G3 and G5, and G4 and G6, respectively. The system can also be seen as two big areas between the Northern area represented by generators G1-G2, and the Central-Southern areas expressed by generators G3-G6, interconnected through two long parallel 500 kV lines.

The linearized model of the system allows to identify the electromechanical oscillations of interest and participation factors associated with the angle and speed states. The system is stable, since all real parts of the eigenvalues are negative. The right eigenvectors (mode shapes), which correspond to the changes in generator rotor speed or angle, show whether a mode is local or inter-area. Inspecting the components of the speed in the right eigenvector associated to the $\lambda_i = -0.6709 \pm j4.2919$ oscillation mode shows that the oscillation with the frequency of $f_i = 0.683$ Hz and damping ratio of $\zeta_i = 0.154$ is an inter-area mode as the generators in the Northern area (G1-G2) swing against those of the Central and Southern areas (G3-G6). The inter-area mode damping should be increased to be higher than 15%.

B. ETDs and Delay Requirements

To determine the ICT delay requirements for wide-area damping controllers, it is assumed that TCSCs are installed in the Vietnamese system, and power oscillation dampers will be installed to add damping to the inter-area mode. The following three cases are considered:

Case (A) : single TCSC 1 using a RI signal ($\delta_1 - \delta_6$) – the phase angle difference between the terminal voltages of generators G1 and G6.

Case (B) : single TCSC 2 using a RI signal ($\delta_1 - \delta_3$) – the phase angle difference between the terminal voltages of generators G1 and G3.

Case (C) : coordination of TCSC 1 using the remote signal ($\delta_1 - \delta_6$) and TCSC 2 using the remote signal ($\delta_1 - \delta_3$).

The TCSC installations are assumed as shown in Fig. 12. Table III indicates the ETD calculation results. The curves in Fig. 13 show the ICT delays for inter-area damping improvement for the three cases.

Fig. 13 is meaningful in selecting a WACS corresponding to required damping improvement. Note from the figure that case (B) offers the lowest damping enhancement capabilities. This is because its curve is the lowest among the three cases. This is in part due to the fact that signal $\delta_1 - \delta_3$ has lower modal content for damping enhancement. If the required damping improvement of the system is less than 11%, the required latency of the ICT system can be higher than 236 ms, and case (A) offers a better choice. In this case, the maximum ICT delay is 753 ms. If the required damping improvement is in a range from 11% to 30%,

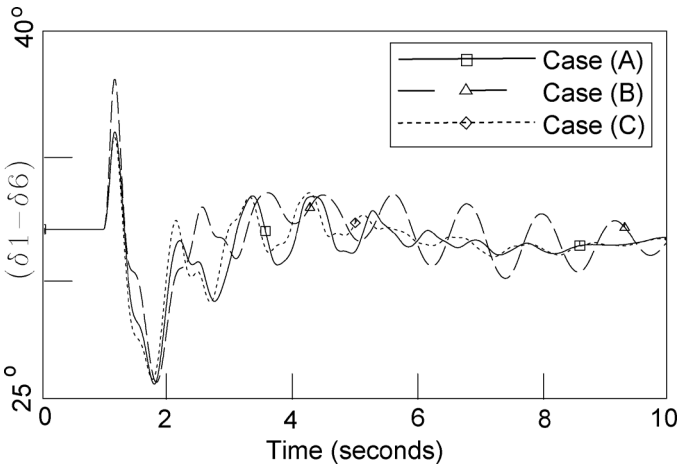

Fig. 14. Nonlinear time-domain simulations corresponding to the three cases using TCSC. The ICT delay of the wide-area measurement is set to 236 ms.

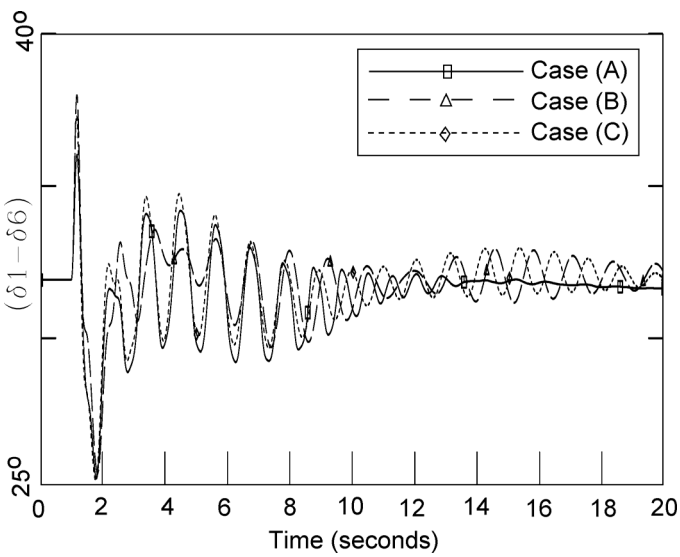

Fig. 15. Nonlinear time-domain simulations corresponding to the three cases using TCSC. The ICT delay of the wide-area measurement is set to 401 ms.

case (C) is a better option, and the ICT delay is required in a range of 236–51 ms.

Observe that the use of two wide-area controllers and their coordination allows for a larger damping enhancement; however, larger damping enhancement also requires a lower value for the maximum delay allowed.

C. Nonlinear Analysis

Nonlinear simulations using a detailed power system of Vietnam (320 buses, 153 generators) are carried out to test the linear analysis results for ICT delay requirements. It is assumed that a three-phase to ground fault $\mathbf{N}$ (Fig. 12) occurs on 500 kV busbar Da Nang, and lasts for 100 ms. Cases (A), (B), and (C) are used to improve inter-area damping using TCSCs. Figs. 14 and 15 show the inter-area damping comparisons in the three cases when the ICT delays are 236 ms and 401 ms, respectively.

When the time delay is 236 ms (Fig. 14), Case (A) (TCSC 1 using RI signal $[\delta_1 - \delta_6)]$ and Case (C) (coordination of two TCSCs) offer the same damping improvement, and outperform to Case (B) [TCSC 2 using RI signal $(\delta_1 - \delta_3)$].

Fig. 15 shows a damping comparison when the time delay is taken as 401 ms. Note that at this latency, only Case (A) ensures the required damping improvement [Case (C) is marginally stable]. Above nonlinear analysis results confirm the validity of the computed allowed ICT delays for the Vietnamese system using the proposed methodology in Section V-B.

VI. Conclusion

The possibility to use remote input signals to dampen power system oscillations and their superiority over local input controllers is well documented. However, remote input signals need to compete with simpler and cheaper controllers that make use of local input signals.

When using remote input signals, the controller needs to at least match the performance of the controller that uses local input signals. In wide-area power system damping control applications, ICT delay requirements for WACS's designs can be defined by a systematic method. This paper defines an Equivalent Time Delay (ETD) and an equivalent time delay for improved damping ($\mathrm{ETD}^{x\,\%}$). This method is a useful to compare different control designs and to define the requirements for the ICT infrastructure. It also allows the grid operator to select appropriate remote input signals to utilize in WACS design.

Attaining a reduced $\mathrm{ETD}^{x\,\%}$ will most likely involve increased capital expenditures and operational expenditure costs of the ICT network. Therefore, there exists a relationship between damping enhancement and cost. An optimal ICT design for WACS can be carried out considering these constraints. This will be explored in future work.

Acknowledgment

N. T. Anh would like to thank the Belgian Technical Cooperation for granting him a scholarship to carry out his Ph.D. studies at the KU Leuven, Belgium.

References

[1] M. Klein, G. J. Roger, and P. Kundur, "A fundamental study of inter-area oscillations," *IEEE Trans. Power Syst.*, vol. 6, no. 3, pp. 914–921, Aug. 1991.

[2] M. E. Aboul-Ela, A. A. Sallam, J. D. McCalley, and A. A. Fouad, "Damping controller design for power system oscillations using global signals," *IEEE Trans. Power Syst.*, vol. 11, no. 2, pp. 767–773, May 1996.

[3] G. Rogers, *Power System Oscillations*. Boston, MA, USA: Kluwer, 2000.

[4] N. Yang, Q. Liu, and J. D. MacCalley, "TCSC controller design for damping interarea oscillations," *IEEE Trans. Power Syst.*, vol. 13, no. 4, pp. 1304–1310, Nov. 1998.

[5] J. H. Chow, J. J. Sanchez-Gasca, H. Ren, and S. Wang, "Power system damping controller design-using multiple input signals," *IEEE Control Syst. Mag.*, vol. 20, no. 4, pp. 82–90, Aug. 2000.

[6] R. M. Mathur and R. K. Varma, *Thyristor-Based FACTS Controllers for Electrical Transmission Systems*. New York, NY, USA: Wiley-Interscience/IEEE Press, 2002.

[7] D. Dotta, A. S. Silva, and I. C. Decker, "Wide-area measurements-based two-level control design considering signal transmission delay," *IEEE Trans. Power Syst.*, vol. 24, no. 1, pp. 208–216, Feb. 2009.

[8] W. Yao, L. Jiang, Q. H. Wu, J. Y. Wen, and S. J. Cheng, "Delay-dependent stability analysis of the power system with a wide-area damping controller embedded," *IEEE Trans. Power Syst.*, vol. 26, no. 1, pp. 233–240, Feb. 2011.

[9] N. T. Anh, D. Van Hertem, and J. Driesen, "Effectiveness of TCSC controllers using remote input signals for transient stability enhancement," in *Proc. IEEE Trondheim PowerTech 2011*, Jun. 2011, pp. 1–8.
[10] Y. Chompoobutrgool and L. Vanfretti, "Identification of power system dominant inter-area oscillation paths," *IEEE Trans. Power Syst.*, vol. 28, no. 3, pp. 2798–2807, Aug. 2013.
[11] J. H. Chow and S. G. Ghiocel, "Control and optimization methods for electric smart grids," in *An Adaptive Wide-Area Power System Controller using Synchrophasor Data*. New York, NY, USA: Springer, 2012, vol. 3, Power Electronics and Power Systems, 2012, pt. 3, pp. 327–342.
[12] D. E. Bakken, A. Bose, C. H. Hauser, D. E. Whitehead, and G. C. Zweigle, "Smart generation and transmission with coherent real-time data," *Proc. IEEE*, vol. 99, no. 6, pp. 928–951, Jun. 2011.
[13] C. W. Taylor, M. V. Venkatasubramanian, and Y. H. Chen, "Wide-area stability and voltage control," in *Proc. VII Symp. Specialists in Electric Operational and Expansion Planning*, 2000.
[14] B. Naduvathuparambil, M. C. Valenti, and A. Feliachi, "Communication delays in wide area measurement systems," in *Proc. 34th Southeastern Symp. System Theory, 2002*, 2002, pp. 118–122.
[15] C. F. M. Danielson, L. Vanfretti, M. S. Almas, Y. Choompoobutrgool, and J. O. Gjerde, "Analysis of communication network challenges for synchrophasor-based wide-area applications," in *Proc. IREP 2013*, Greece, Aug. 25–30, 2013.
[16] Y. Chompoobutrgool and L. Vanfretti, "A fundamental study on damping control design using PMU signals from dominant inter-area oscillation paths," in *Proc. 2012 North Amer. Power Symp., NAPS 2012*, Sep. 2012.
[17] L. Vanfretti, Y. Chompoobutrgool, and J. H. Chow, "Coherency and model reduction of large power systems," in *Inter-Area Mode Analysis for Large Power Systems Using Synchrophasor*, J. H. Chow, Ed. New York, NY, USA: Springer, 2013, ch. 10.
[18] N. Martins and L. T. G. Lima, "Determination of suitable locations for power system stabilizers and static var compensators for damping electromechanical oscillations in large scale power systems," *IEEE Trans. Power Syst.*, vol. 5, no. 4, pp. 1455–1469, Nov. 1990.
[19] H. F. Wang, F. J. Swift, and M. Li, "Selection of installing locations and feedback signals of FACTS-Based stabilizers in multimachine power systems by reduced-order modal analysis," *Proc. Inst. Elect. Eng., Gen. Transm. Distrib.*, vol. 144, no. 3, pp. 263–269, May 1997.
[20] L. Rouco and F. L. Pagola, "An eigenvalue sensitivity approach to location and controller design of controllable series capacitors for damping power system oscillations," *IEEE Trans. Power Syst.*, vol. 12, no. 4, pp. 1660–1666, Nov. 1997.
[21] P. Pourbeik and M. J. Gibbard, "Damping and synchronizing torques induced on generators by FACTS stabilizers in multimachine power systems," *IEEE Trans. Power Syst.*, vol. 11, no. 4, pp. 1920–1925, Nov. 1996.
[22] S. E. M. De Oliveira, "Synchronizing and damping torque coefficients and power system steady-state stability as affected by static VAR compensators," *IEEE Trans. Power Syst.*, vol. 9, no. 1, pp. 109–119, Feb. 1994.
[23] B. T. Ooi, M. Kazerani, R. Marceau, Z. Wolanski, F. D. Galiana, D. McGillis, and G. Joos, "Mid-point siting of FACTS devices in transmission lines," *IEEE Trans. Power Del.*, vol. 12, no. 4, pp. 1717–1722, Oct. 1997.
[24] M. M. Farsangi, Y. H. Song, and K. Y. Lee, "Choice of FACTS device control inputs for damping interarea oscillations," *IEEE Trans. Power Syst.*, vol. 19, no. 2, pp. 1135–1143, May 2004.
[25] Y. Chang, Z. Xu, G. Cheng, and J. Xie, "A novel SVC supplementary controller based on wide area signals," in *Proc. IEEE Power Eng. Soc. General Meeting, 2006*, 2006.
[26] N. T. Anh, "Damping controller design with PMU feedback input signals and TCSC applications to the Vietnamese network," Ph.D. dissertation, KU Leuven, Leuven, Belgium, 2013.

Nguyen Tuan Anh was born in 1973 in Hanoi, Vietnam. He received the B.S. and M.Sc. degrees in electrical engineering from Hanoi University of Technology, Vietnam, in 1995 and 2004, respectively, and the D.Eng. degree from the KU Leuven, Belgium, in 2013.

His research interests are flexible AC transmission system (FACTS) and power system stability and control.

Luigi Vanfretti (S'03–M'10–SM'14) received the electrical engineering degree from Universidad de San Carlos de Guatemala, Guatemala City, Guatemala, in 2005, and the M.Sc. and Ph.D. degrees in electric power engineering from Rensselaer Polytechnic Institute, Troy, NY, USA, in 2007 and 2009, respectively.

He was a Visiting Researcher with The University of Glasgow, Glasgow, U.K., in 2005. He became an Assistant Professor with the Electric Power Systems Department, KTH Royal Institute of Technology, Stockholm, Sweden, in 2010 and was conferred the Swedish title of "Docent" in 2012. He is currently a tenured Associate Professor with the same department. He is Special Advisor in Strategy and Public Affairs for the Research and Development Division of Statnett SF, the Norwegian transmission system operator. His duties include architectural analysis for synchrophasor data transfer, communications, and application systems to be utilized in Smart Transmission Grid applications; as well as providing inputs into R&D strategy development and aiding in the execution of collaborative projects with universities, TSOs, and R&D providers. He is an advocate for free/libre and open-source software. His research interests are in the general area of power system dynamics; while his main focus is on the development of applications of PMU data.

Dr. Vanfretti has served, since 2009, in the IEEE Power Engineering Society (PES) PSDP Working Group on Power System Dynamic Measurements, where he is now the Chair. In addition, since 2009, he has served as Vice-Chair of the IEEE PES CAMS Task Force on Open Source Software. For his research and teaching work toward his Ph.D. degree, he was awarded the Charles M. Close Award from Rensselaer Polytechnic Institute.

Johan Driesen (S'93–M'97–SM'12) was born in 1973 in Belgium. He received the M.Sc. degree in 1996 as Electrotechnical Engineer from the KU Leuven, Belgium. He received the Ph.D. degree in Electrical Engineering at K.U.Leuven in 2000 on the finite element solution of coupled thermalelectromagnetic problems and related applications in electrical machines and drives, microsystems and power quality issues.

Currently he is a full professor at the KU Leuven and teaches power electronics and drives. In 2000–2001 he was a visiting researcher in the Imperial College of Science, Technology and Medicine, London, U.K. In 2002 he was working at the University of California, Berkeley, CA, USA. Currently he conducts research on distributed generation, including renewable energy systems, power electronics and its applications, for instance in drives and power quality.

Dirk Van Hertem (S'02–SM'09) was born in 1979 in Neerpelt, Belgium. He received the M.Eng. degree from the KHK, Geel, Belgium, in 2001 and the M.Sc. degree in electrical engineering from the KU Leuven, Belgium, in 2003. In 2009, he received the Ph.D. degree, also from the KU Leuven.

In 2010, he was a member of EPS group at the Royal Institute of Technology, Stockholm, Sweden, where he was the program manager for controllable power systems for the EKC^2 competence at KTH. Since spring 2011 he is back at the University of Leuven where he is an Assistant Professor in the ELECTA group. His special fields of interest are power system operation and control in systems with HVDC and FACTS and building the transmission system of the future, including offshore grids and the supergrid concept.

Dr. Van Hertem is an active member of both IEEE (PES and IAS) and Cigré.